

# Recent Dynamical Evolution of Galaxy Clusters

M. Plionis

*Instituto Nacional de Astrofisica, Optica y Electronica (INAOE), Apartado Postal 51 y  
216, 72000, Puebla, Pue., Mexico*

*and*

*Institute of Astronomy & Astrophysics, National Observatory of Athens, I.Metaxa &  
B.Pavlou, P.Penteli 152 36, Athens, Greece*

## ABSTRACT

Evidence is presented for a recent evolution of the relaxation processes in clusters of galaxies, using large optical and X-ray cluster samples. The criteria of the cluster relaxation used are the cluster ellipticity, the ICM temperature and X-ray cluster luminosity. We find evidence of varying strength and significance of all three indicators evolving with redshift for  $z \lesssim 0.15$ . This result supports the view that clusters have mostly stopped undergoing mergers and accreting matter, as expected in a low- $\Omega_m$  Universe, and are now in the process of gravitational relaxation, which reduces their flattening, their ICM temperature (shock heated during the merging phase), and their X-ray luminosity. These results support similar recent claims of Melott, Chambers and Miller.

*Subject headings:* galaxies: clusters: general - galaxies: evolution -large-scale structure of universe

## 1. Introduction

The present dynamical state of clusters of galaxies should contain interesting cosmological information since the rate of growth of perturbations is different in universes with different matter content (Peebles 1980); in an  $\Omega_m = 1$  universe the perturbations grow proportionally to the scale factor [ $\delta \propto (1+z)^{-1}$ ], while in the extreme case of an empty universe, they do not grow at all [ $\delta = \text{constant}$ ]. It is also known that  $\Omega_m < 1$  universes behave dynamically as an  $\Omega = 1$  universe at large redshifts, while at some redshift  $z \simeq \Omega_m^{-1} - 2$  perturbations stop evolving, allowing clusters to relax up to the present epoch much more than in an  $\Omega_m = 1$  model, in which clusters are still forming.

Note that a flat  $\Omega_\Lambda > 0$  model behaves as an  $\Omega_m = 1$  model up to a lower redshift than the corresponding open model, while for redshifts  $z \lesssim 1$  it behaves like an open model

(Lahav et al. 1991). This implies that clusters even in this model should be dynamically older than in an EdS model (Richstone et al. 1992; Evrard et al. 1993; Lacey & Cole 1996; Beisbart, Valdarnini & Buchert 2002; Suwa et al. 2002).

Therefore one should be able to put constraints on  $\Omega$  from the evolution of the cluster dynamical state. One such indicator, the cluster ellipticity, was recently proposed in Melott et al. (2001); the more elliptical a cluster the younger it is, since ellipticity should be correlated with the anisotropic accretion of matter and merging (e.g., Buote 1998; Kolokotronis et al. 2001). Melott et al. (2001) presented evidence for a recent evolution ( $z \lesssim 0.1$ ) of cluster ellipticity, defined in both optical and X-ray bands, based on various cluster samples, containing in total  $\sim 160$  rich Abell clusters. An earlier study, using clusters identified in the Lick map (Plionis et al. 1991), had also found that cluster ellipticity decreases with redshift for  $z \lesssim 0.1$ , due however to possible systematic effects involved in the construction of the data, the authors did not attach much weight to this result.

This interesting finding was interpreted in Melott et al. (2001) as an indication of a low- $\Omega_m$  universe, because in such a universe and under the hierarchical clustering scenario, one expects that merging and anisotropic accretion of matter along filaments (Shandarin & Klypin 1984) will have stopped long ago. Thus the clusters should be relatively isolated and gravitational relaxation will tend to isotropize the clusters reducing their ellipticity, more so in the recent times. A variety of indications do exist supporting the formation of clusters by hierarchical aggregation of smaller units along filamentary large-scale structures (e.g. West, Jones & Forman 1995; Plionis & Basilakos 2002).

Although the cluster ellipticity is a relatively well defined quantity, systematic effects due to projections in the optical, that could increase the ellipticity of spherical clusters or decrease the ellipticity of flat ones, or the strong central concentration of the X-ray emitting gas (since  $L_x \propto n_e^2$ ) in the X-ray band, which in conjunction with resolution effects could reduce the ellipticity of distant clusters, should be taken into account. One should therefore use large and well constructed samples of galaxy clusters to verify such an ellipticity trend. Furthermore, other indicators of recent cluster evolution should be used as well. For example, if the ellipticity decrease with  $z$  is indeed due to recent dynamical relaxation processes, then one should expect an evolution of the temperature of the X-ray emitting gas as well as the X-ray cluster luminosity which should follow the same trend as the cluster ellipticity, decreasing at recent times, since the violent merging events, at relatively higher redshifts, will compress and shock heat the diffuse ICM gas (e.g., Ritchie & Thomas 2002). Another possible indicator could be the cluster velocity dispersion, which naively one would expect to increase at lower redshifts, since virialization will tend to increase the cluster ‘thermal’ velocity dispersion. Although there is a quite well defined  $L_x - \sigma$  relationship (e.g., Quintana

& Melnick 1982; White et al. 1997), unrelaxed clusters can also show up as having a high velocity dispersion due to either possible large peculiar velocities of the different sub-clumps (e.g., Rose et al. 2002) or due to the possible sub-clump virialized nature. Therefore, a better physical understanding of the merging history of clusters is necessary in order to be able to utilize the velocity dispersion measure as an evolution criterion.

In this letter, we will present further evidence for a recent dynamical evolution of clusters, using the optical APM and the X-ray XBAC and BCS cluster samples and three indicators of cluster dynamical evolution, namely ellipticity, the X-ray cluster temperature and X-ray luminosity.

## 2. Data

Details of the APM cluster sample and its construction can be found in Dalton et al. (1997). Here we only remind the reader that the APM cluster catalogue is based on the APM galaxy survey, which covers an area of 4300 square degrees in the southern sky and contains about 2.5 million galaxies brighter than a magnitude limit of  $b_J = 20.5$  (Maddox et al. 1990). Dalton et al. (1997) applied an objective cluster finding algorithm to the APM galaxy data using a search radius of  $0.75 h^{-1}$  Mpc, in order to minimize projection effects, and so produced a list of 957 clusters with  $z \lesssim 0.15$ . Out of these 309 ( $\sim 32\%$ ) are ACO clusters, while 407 ( $\sim 45\%$ ) have measured redshifts. The APM clusters that are not in the ACO list are relatively poorer systems than the Abell clusters, as can be verified comparing their mean APM richness's, determined in Dalton et al. (1997).

The APM cluster shape parameters (ellipticity and position angles) were estimated in Basilakos et al. (2000) and were used to measure the intrinsic distribution of clusters shapes (found to be prolate-like). The shape parameters were estimated using the moments of inertia method on the Gaussianly smoothed galaxy distribution, the angular smoothing scale of which depends on the distance of each cluster. An optimum grid size was selected based on an extensive Monte-Carlo procedure. In order not to bias the ellipticity measurements no circular aperture was used, but rather all cells above a selected density threshold were feed into the inertia tensor. Three such thresholds were used to provide the shape parameters at three different scales and to test their robustness as a function of distance from the cluster center [see details in Basilakos et al. (2000) and Kolokotronis et al. (2001)]. The shape parameters for all APM clusters as well as indicators of the dynamical state of each APM cluster will be published shortly (Plionis & Basilakos in preparation).

Here we will use the ellipticities of 903 APM clusters that have measured shape param-

eters (54 clusters are found in the vicinity of plate-holes or crowded regions and thus are excluded). We will also use the XBAC (Ebeling et al. 1996) and BCS (Ebeling et al. 1998) ROSAT X-ray cluster samples to test whether there is any indications of a recent evolution of the ICM temperature. Details of the sample construction can be found in the original papers. We only note that the XBACs has a flux-limit of  $f_x > 5 \times 10^{-12} \text{ sec}^{-1} \text{ cm}^{-2}$  and contains 283 Abell clusters, while the BCS, with its low-flux extension (Ebeling et al. 2001), has a flux limit of  $f_x > 2.8 \times 10^{-12} \text{ ergs sec}^{-1} \text{ cm}^{-2}$  and contains 304 clusters. Most of the listed ICM temperatures are estimated from the  $L_x - T$  relation of White et al. (1997), but a reasonable number of clusters have measured temperatures [see Table 1 of White et al. (1997)]. The flux-limited nature of these samples create an apparent  $L_x - z$  relation, as can be seen in Figure 1, and in order to avoid reproducing an artificial redshift evolution we construct volume limited subsamples (the delineated regions of Fig.1); one is a low-luminosity ( $L_x > 10^{44} \text{ ergs/sec}$ ) subsample, which spans a limited redshift range ( $z \lesssim 0.07$  and  $0.09$  for the XBACs and BCS, respectively) and one high-luminosity subsample ( $L_x > 8 \times 10^{44} \text{ ergs/sec}$ ), spanning a much larger redshift range ( $z \lesssim 0.19$  and  $0.24$  for the XBACs and BCS, respectively).

### 3. Results & Discussion

Figure 2 shows the distribution of APM cluster ellipticities as a function of redshift ( $z < 0.18$ ). The filled circles represent APM clusters that are also in the Abell/ACO catalogue. There is a definite trend of ellipticity with redshift in the direction expected from an evolution of the dynamical status of clusters, supporting similar claims of Melott et al. (2001). Table 1 summarizes the quantitative correlation results for all tests. The Pearson correlation coefficient for the  $\epsilon - z$  correlation is  $r \simeq 0.2$  and with a probability of being a chance correlation of  $\mathcal{P} \simeq 10^{-8}$ . This result is robust to changes of the sample size by factors of two or three, depending on whether we use clusters with observed redshifts or different cluster richness (see Table 1).

Tests were performed to investigate whether systematic effects in the shape-parameter determination method could be responsible for the ellipticity-redshift trend. Already in Basilakos et al. (2000) a detailed analysis of the performance of the method as a function of sampling, distance and the presence of a projected random background galaxy distribution [as predicted by the luminosity function of APM galaxies; Maddox et al. (1996)] showed that such effects will tend to overestimate by  $\sim 0.1 - 0.15$  the ellipticity of nearly spherical clusters (more so for distant clusters - but only by 5% more), they will underestimate the ellipticity of flat clusters, more so at large-redshifts, while they will leave unaffected the

clusters with ellipticities around the mean of the distribution (ie.,  $\epsilon \sim 0.4$ ). These effects could in principle bias the ellipticity redshift correlation, depending on the relative abundance of different ellipticity clusters. We investigate this possibility by performing a Monte-Carlo simulation analysis in which we assume the same underlying cluster ellipticity distribution at all redshifts. Then using the individual APM cluster distance and richness characteristics we simulate, for each APM cluster, 1000 mock clusters having ellipticities derived by randomly sampling the corrected, for different biases, ellipticity distribution [see Fig.6 of Basilakos et al. (2000)]. Mock clusters are constructed having King profiles and the APM richness at the selected distance from the observer as in Basilakos et al. (2000). The estimated background is overlaid on the cluster image, allowing however for clustering (we take the extreme case that all the background galaxies are clustered at the distance of the cluster). From the resulting population of  $\sim 900000$  cluster ellipticities, which have the correct underlying APM redshift selection function, we randomly select  $N$ -times 900 ellipticities and estimate their correlation with redshift ( $N = 40000$ ). We find no significant correlation (ie.,  $\langle r \rangle = 0.08$  and  $\langle \mathcal{P} \rangle = 0.08$ ), while only in 16 out of the 40000 cases do we find a similar  $\epsilon - z$  correlation having the observed, or higher significance level. This number drops to 3 if we use a random, instead of a clustered, background in the mock cluster construction. Since we have used the extreme case where all the background is assumed to be clustered at the distance of each APM cluster, we should consider the derived significance as an upper limit. Therefore the true significance of the observed  $\epsilon - z$  correlation, taking into account the possible redshift dependent systematic effects, is

$$\mathcal{P}_{\epsilon-z} \lesssim 4 \times 10^{-4} ,$$

verifying that our ellipticity determination method, coupled with shot-noise and the projection of a clustered background cannot create the observed  $\epsilon - z$  trend.

Regarding the  $kT - z$  relation, we have found that there is indeed a correlation, especially apparent in the high- $L$  subsample, which spans a larger range in  $z$  (see Figure 3 and Table 1). The correlation coefficient for the combined XBAC-BCS high- $L$  subsample (were for the common clusters we have used only the more accurate BCS values) is  $r \simeq 0.47$  with probability of chance correlation being  $\mathcal{P} \simeq 3 \times 10^{-4}$ . This correlation is also apparent in each individual cluster sample as well, although with a slightly lower significance. A similar but weaker  $kT - z$  correlation is found in the low- $L$  sample.

Note, however, that many of the used temperatures are based on the  $L_x - kT$  relation of White et al. (1997) and thus this correlation could be a manifestation of an underlying  $L_x - z$  relation. In order to investigate this possibility we restrict our analysis only to those clusters with measured temperatures, reducing our samples considerably (by more than 50%), but the correlation of  $kT$  with  $z$  persists (see Table 1). Especially for the low- $L_x$  sample the correlation now is even stronger and more significant. For the high- $L$  sample, where the

sample number has dropped by a factor of 3, there is still an apparent correlation but the significance has dropped considerably. Therefore, we confirm that cluster temperatures do evolve with redshift in the recent past.

We return to the question of a possible recent  $L_x$  evolution, which if present it could extend, through the  $L_x - kT$  relation, the already existing  $kT - z$  relation also to clusters with estimated temperatures. Indeed, as seen in Figure 4, where we plot the  $L_x$  versus  $z$  (see also Table 1), we do find such a relation with correlation coefficient  $r \simeq 0.4$  and significance  $\mathcal{P} \sim 0.003 - 0.14$  (depending on the subsample). Note, however, that if we use all the clusters in our subsample (not only those with measured temperatures) then we observe a correlation only for the high- $L_x$  sample ( $r \simeq 0.2$ ) which is weak and of low significance ( $\mathcal{P} \sim 0.15$ ). It could be that clusters with measured temperatures have more accurately measured luminosities.

### 3.1. Conclusions

We have presented evidence, based on the optical APM and X-ray XBAC and BCS cluster samples, of a recent dynamical evolution of clusters, a fact to be expected if in clusters the merging and anisotropic accretion of matter along filaments have stopped and relaxation processes are now in effect. Gravitational relaxation will tend to isotropize the clusters reducing their ellipticity, their ICM temperature (shock heated during the violent merging phase of their formation) and their X-ray luminosity. We have found indications of varying strength and significance for all three of these effects, supporting similar claims of Melott et al. (2001), on the basis of an ellipticity-redshift relation. These results appear to be consistent with the expectations of a low- $\Omega_m$  Universe.

I would like to thank Adrian Melott for a discussion.

### REFERENCES

- Basilakos, S., Plionis, M., Maddox, S., 2000, MNRAS, 316, 779  
 Beisbart, C., Valdarnini, R., Buchert, T., 2002, A&A, 379, 412  
 Buote, D.A., 1998, MNRAS, 293, 381  
 Dalton G. B., Maddox S. J., Sutherland W. J., Efstathiou G., 1997, MNRAS, 289, 263

- Ebeling, H., Voges, W., Böhringer, H., Edge, A.C., Huchra, J.P. and Briel, U.G., 1996, MNRAS, 281, 799
- Ebeling, H., Edge, A.C., Böhringer, H., Allen, S.W., Crawford, C.S., Fabian, A.C., Voges, W., Huchra, J.P., 1998, MNRAS, 301, 881
- Ebeling, H., Edge, A.C., Allen, S.W., Crawford, C.S., Fabian, A.C., Huchra, J.P., 2001, MNRAS, 318, 333
- Evrard A.E., Mohr J.J., Fabricant D.G., Geller M.J., 1993, ApJ, 419, L9
- Kolokotronis, V., Basilakos, S., Plionis, M., Georgantopoulos, 2001, MNRAS, 320, 49
- Lacey, C., Cole, S., 1996, MNRAS, 262, 627
- Lahav, O., Rees, M.J., Lilje, P.B., Primack, J., 1991, MNRAS, 251, 128
- Maddox S.J., Sutherland W.J., Efstathiou G., Loveday, J. 1990, MNRAS, 243, 692
- Maddox S.J., Efstathiou, G., Sutherland W.J., 1996, MNRAS, 283, 1227
- Melott, A.L., Chambers, S.W., Miller, C.J., 2001, ApJ, 559, L75
- Peebles, P.J.E., 1980, *Physical Cosmology*, Princeton Univ. Press
- Plionis, M, Barrow, J.D. & Frenk, C.S. 1991, MNRAS, 249, 662
- Plionis, M. & Basilakos, S., 2002, MNRAS, 329, L47
- Quintana, H. & Melnick, J. 1982, AJ, 87, 972
- Richstone, D., Loeb, A., Turner, E.L., 1992, ApJ, 393, 477
- Ritchie, B.W., Thomas, P.A., 2002, MNRAS, 329, 675
- Rose, J.A., Gaba, A.E., Christiansen, W.A., Davis, D.S., Caldwell, N., Hunstead, R.W., Johnston-Hollitt, M., 2002, AJ, 123, 1216
- Shandarin, S.F. & Klypin, A., 1984, Soviet Ast.28, 491
- Suwa, T., Habe, A., Yoshikawa, K., Okamoto, T., 2002, ApJ, in press, *astro-ph/0108308*
- West, M.J., Jones, C., & Forman, W., 1995, ApJ, 451, L5
- White, D. A., Jones, C., Forman, W., 1997, MNRAS, 292, 419

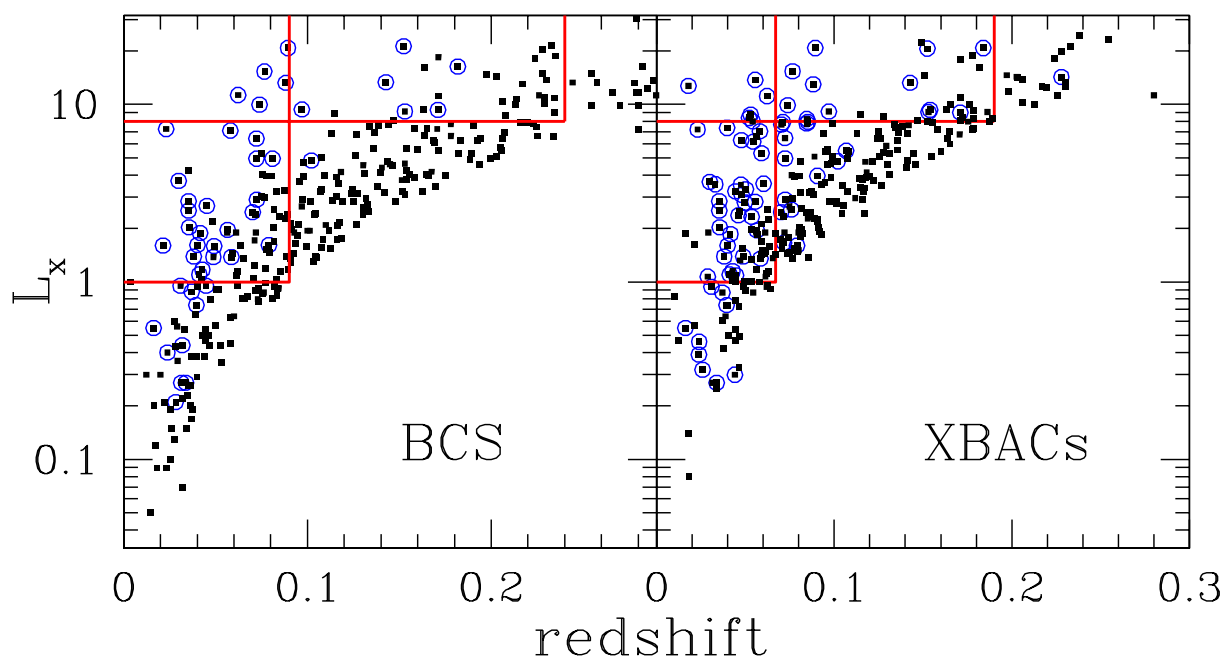


Fig. 1.— The X-ray Luminosity-redshift plot for the BCS and XBAC samples. The strong dependence of  $L_x$  on  $z$  due to the flux limit is apparent. Open circles represent clusters with observed temperatures from White et al. (1997) and the delineated regions represent the volume-limited subsamples analysed.



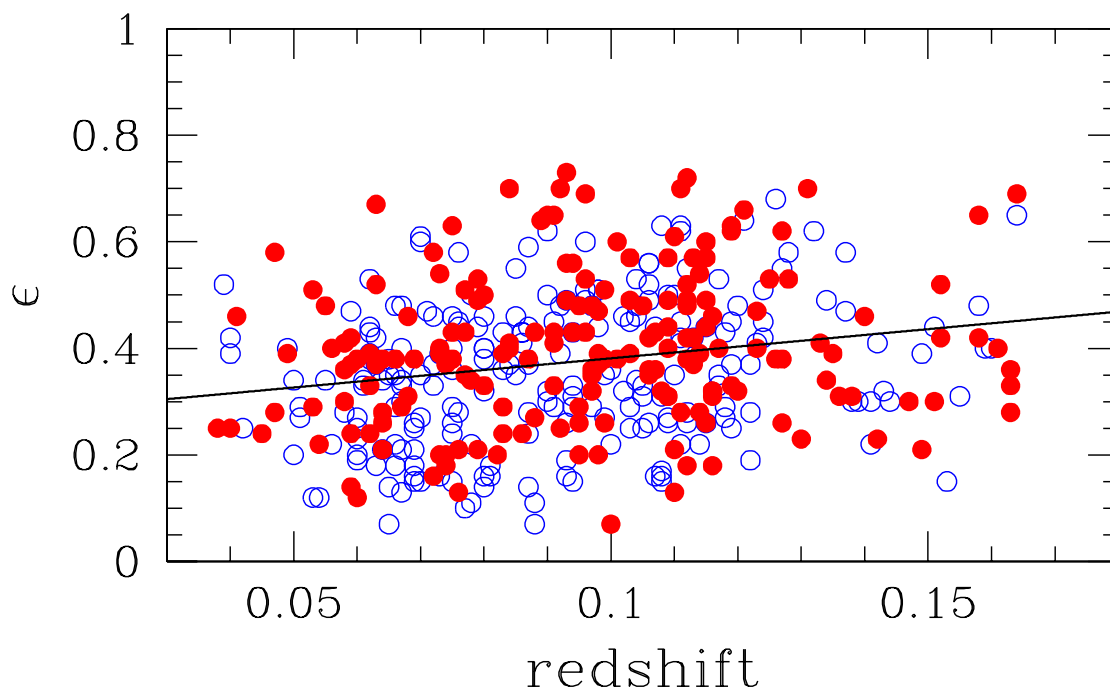


Fig. 2.— The evolution with redshift of the APM cluster ellipticity. For clarity only clusters with measured redshifts are presented. Filled circles are those APM clusters that are also in the Abell/ACO sample. The straight line represented the best least-square fit to the data.

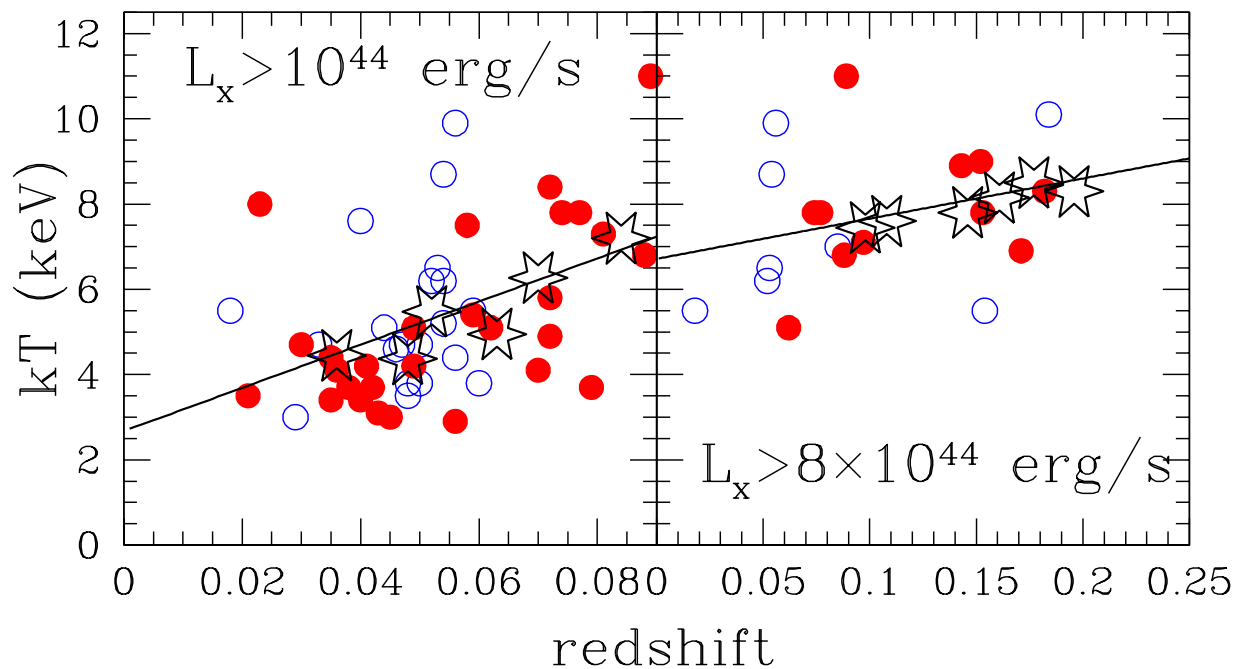


Fig. 3.— The ICM temperature redshift correlation for the two subsamples analysed. Filled and open points represent BCS and XBAC clusters, respectively. The solid line is the best least-square fit to the data, while the stars represent the mean ICM temperature in equal volume shells (3 shells for each sample, plotted together). Note that we plot only those clusters with measured temperatures from White et al. (1997) (those having errorbars in their Table 1).

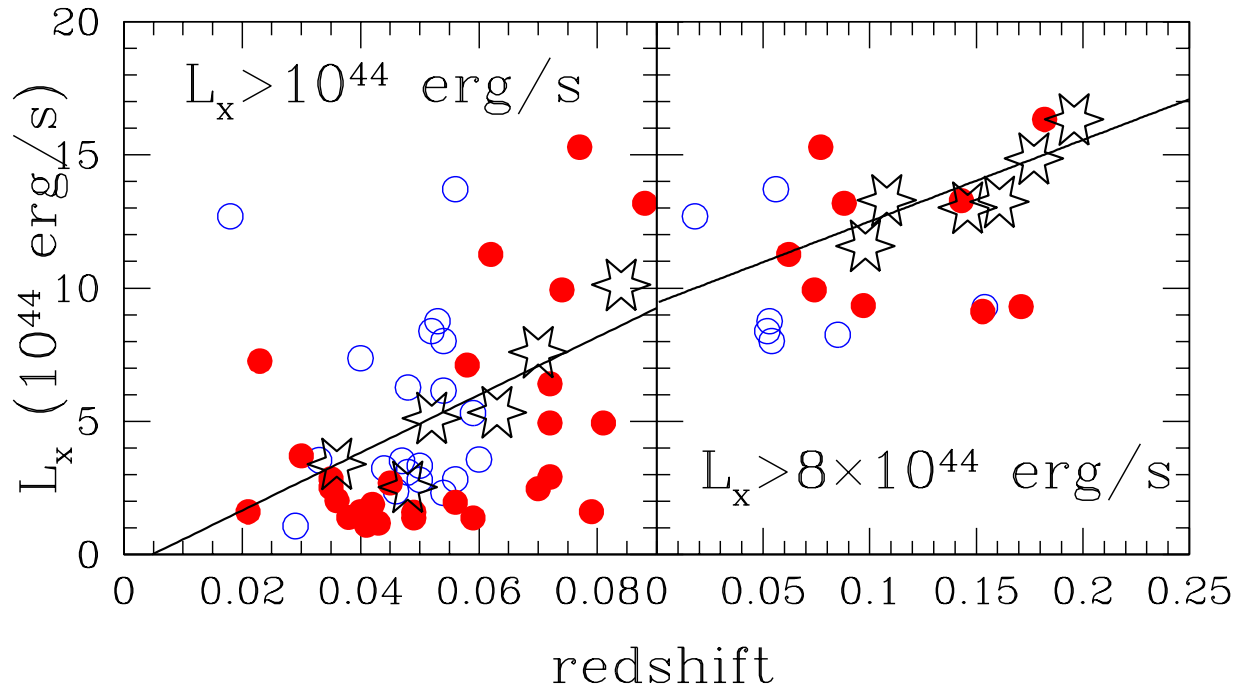


Fig. 4.— The X-ray luminosity ( $L_x$ ) redshift correlation for the two subsamples analysed. Symbols are as in figure 3.

Table 1. Correlation analysis results for the different correlation pairs and samples.

Cluster sample	$N$	correlation pair	$r$	$\mathcal{P}$
APM ( $z_{\text{lim}} \sim 0.18$ )	899	$\epsilon - z$	0.19	$4.3 \times 10^{-9}$
APM ( $z_{\text{obs}}$ )	404	$\epsilon - z$	0.22	$9.6 \times 10^{-6}$
APM ( $> 50$ counts)	411	$\epsilon - z$	0.21	$2.8 \times 10^{-5}$
BCS+XBACs (high- $L_x$ )	55	$kT - z$	0.47	$1.3 \times 10^{-4}$
BCS+XBACs (low- $L_x$ )	106	$kT - z$	0.16	$7.5 \times 10^{-2}$
BCS+XBACs (high- $L_x$ ) meas.	19	$kT - z$	0.30	0.22
BCS+XBACs (low- $L_x$ ) meas.	48	$kT - z$	0.45	$1.5 \times 10^{-3}$
BCS+XBACs (high- $L_x$ ) meas.	19	$L_x - z$	0.36	0.14
BCS+XBACs (low- $L_x$ ) meas.	48	$L_x - z$	0.42	$3 \times 10^{-3}$